A Letters Journal Exploring
the Frontiers of Physics

OFFPRINT

# Interaction of a point charge with the surface of a uniaxial dielectric

Primož Rebernik Ribič and Rudolf Podgornik

EPL, **102** (2013) 24001

Please visit the new website
www.epljournal.org

A LETTERS JOURNAL EXPLORING THE FRONTIERS OF PHYSICS

# AN INVITATION TO SUBMIT YOUR WORK

www.epljournal.org

## The Editorial Board invites you to submit your letters to EPL

EPL is a leading international journal publishing original, high-quality Letters in all areas of physics, ranging from condensed matter topics and interdisciplinary research to astrophysics, geophysics, plasma and fusion sciences, including those with application potential.

The high profile of the journal combined with the excellent scientific quality of the articles continue to ensure EPL is an essential resource for its worldwide audience. EPL offers authors global visibility and a great opportunity to share their work with others across the whole of the physics community.

## Run by active scientists, for scientists

EPL is reviewed by scientists for scientists, to serve and support the international scientific community. The Editorial Board is a team of active research scientists with an expert understanding of the needs of both authors and researchers.


IMPACT FACTOR 2.753*

* As ranked by ISI 2010

www.epljournal.org

epl A LETTERS JOURNAL EXPLORING THE FRONTIERS OF PHYSICS

www.epljournal.org

**IMPACT FACTOR**
**2.753***
* As listed in the ISI® 2010 Science Citation Index Journal Citation Reports

**OVER**
**500 000**
**full text downloads in 2010**

**30 DAYS**
**average receipt to online publication in 2010**

**16 961**
**citations in 2010**
**37% increase from 2007**

*"We've had a very positive experience with EPL, and not only on this occasion. The fact that one can identify an appropriate editor, and the editor is an active scientist in the field, makes a huge difference."*

**Dr. Ivar Martinv**
Los Alamos National Laboratory, USA

## Six good reasons to publish with EPL

We want to work with you to help gain recognition for your high-quality work through worldwide visibility and high citations.

1. **Quality** – The 40+ Co-Editors, who are experts in their fields, oversee the entire peer-review process, from selection of the referees to making all final acceptance decisions
2. **Impact Factor** – The 2010 Impact Factor is 2.753; your work will be in the right place to be cited by your peers
3. **Speed of processing** – We aim to provide you with a quick and efficient service; the median time from acceptance to online publication is 30 days
4. **High visibility** – All articles are free to read for 30 days from online publication date
5. **International reach** – Over 2,000 institutions have access to EPL, enabling your work to be read by your peers in 100 countries
6. **Open Access** – Articles are offered open access for a one-off author payment

Details on preparing, submitting and tracking the progress of your manuscript from submission to acceptance are available on the EPL submission website **www.epletters.net**.

If you would like further information about our author service or EPL in general, please visit **www.epljournal.org** or e-mail us at **info@epljournal.org**.

**EPL is published in partnership with:**

European Physical Society | Società Italiana di Fisica | EDP Sciences | IOP Publishing epl

A Letters Journal Exploring the Frontiers of Physics

# EPL Compilation Index

www.epljournal.org

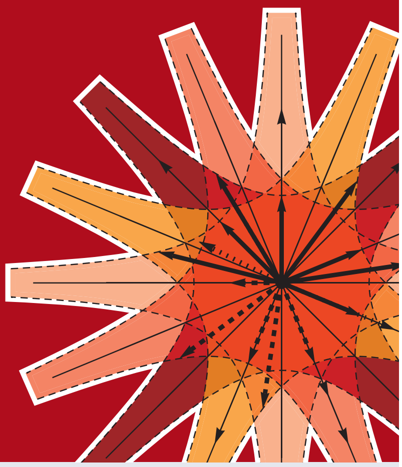

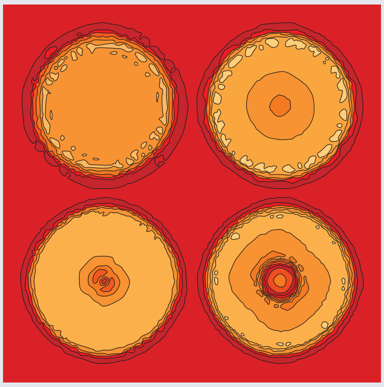

Biaxial strain on lens-shaped quantum rings of different inner radii, adapted from **Zhang *et al*** 2008 EPL **83** 67004.

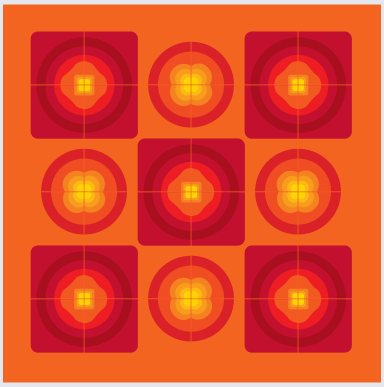

Artistic impression of electrostatic particle–particle interactions in dielectrophoresis, adapted from **N Aubry and P Singh** 2006 *EPL* **74** 623.

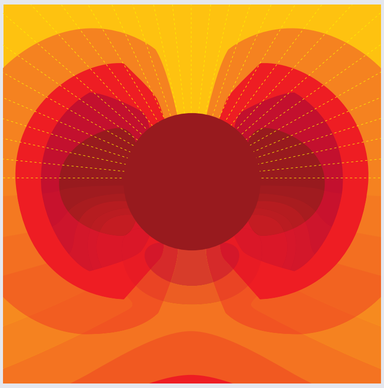

Artistic impression of velocity and normal stress profiles around a sphere that moves through a polymer solution, adapted from **R Tuinier, J K G Dhont and T-H Fan** 2006 *EPL* **75** 929.

Visit the EPL website to read the latest articles published in cutting-edge fields of research from across the whole of physics.

Each compilation is led by its own Co-Editor, who is a leading scientist in that field, and who is responsible for overseeing the review process, selecting referees and making publication decisions for every manuscript.

- Graphene
- Liquid Crystals
- High Transition Temperature Superconductors
- Quantum Information Processing & Communication
- Biological & Soft Matter Physics
- Atomic, Molecular & Optical Physics
- Bose–Einstein Condensates & Ultracold Gases
- Metamaterials, Nanostructures & Magnetic Materials
- Mathematical Methods
- Physics of Gases, Plasmas & Electric Fields
- High Energy Nuclear Physics

If you are working on research in any of these areas, the Co-Editors would be delighted to receive your submission. Articles should be submitted via the automated manuscript system at **www.epletters.net**

If you would like further information about our author service or EPL in general, please visit **www.epljournal.org** or e-mail us at **info@epljournal.org**

EPS Società Italiana di Fisica EDP SCIENCES IOP Publishing

**Image:** Ornamental multiplication of space-time figures of temperature transformation rules (adapted from T. S. Bíró and P. Ván 2010 *EPL* **89** 30001; artistic impression by Frédérique Swist).

A LETTERS JOURNAL EXPLORING THE FRONTIERS OF PHYSICS

April 2013

EPL, **102** (2013) 24001
doi: 10.1209/0295-5075/102/24001

www.epljournal.org

# Interaction of a point charge with the surface of a uniaxial dielectric

PRIMOŽ REBERNIK RIBIČ[1] and RUDOLF PODGORNIK[2]

[1] *Faculté des Sciences de Base, Ecole Polytechnique Fédérale de Lausanne (EPFL) - CH-1015 Lausanne, Switzerland*
[2] *Department of Theoretical Physics, J. Stefan Institute and Department of Physics, Faculty of Mathematics and Physics, University of Ljubljana - SI-1000 Ljubljana, Slovenia, EU*

received on 4 April 2013; accepted by B. A. van Tiggelen on 7 April 2013
published online 18 April 2013

PACS 41.20.-q – Applied classical electromagnetism
PACS 41.60.-m – Radiation by moving charges
PACS 41.75.-i – Charged-particle beams

**Abstract** – We analyze the force on a point charge moving at relativistic speeds parallel to the surface of a uniaxial dielectric. Two cases are examined: a lossless dielectric with no dispersion and a dielectric with a plasma-type response. The treatment focuses on the peculiarities of the strength and direction of the interaction force as compared to the isotropic case. We show that a plasma-type dielectric can, under specific conditions, repel the point charge.

editor's choice Copyright © EPLA, 2013

**Introduction.** – Despite the long and rich history of theoretical studies on the interaction between fast charges and solid surfaces (see, *e.g.* refs. [1–12]) unexpected results can be and indeed are derived. A recent example is the discovery by one of the authors of the present letter [13], that the interaction between a relativistic charge packet and a metal or dielectric surface can become repulsive by simply tuning the packet geometry; a result that seems to go against common notions established in electrodynamics and should be of importance in the framework of accelerator physics and electron spectroscopy.

In this letter we switch gears and focus on the interaction between a point charge and a uniaxial dielectric within the context of ionic and molecular interactions with macroscopic surfaces. We assume a description of the surface that approximates the non-isotropic nature of crystalline surfaces and surfaces decorated with adsorbed non-isotropic inclusions. We present a derivation of the force on the charged particle starting from Maxwell's equations in Fourier space and then evaluate the force numerically in real space. We show that the longitudinal component of the force (parallel to the dielectric surface) is in general not parallel to the particle velocity anymore and that its direction depends on the particle speed (energy). We demonstrate two peculiarities of the plasma-type response: 1) the direction of the longitudinal force depends on the distance of the particle from the surface and 2) under specific conditions the particle can be repelled by the surface.

**Evaluation of the electromagnetic force.** – The geometry of the problem is illustrated in fig. 1. A point charge moves in vacuum with a velocity $\mathbf{v}$ at a distance $z_0$ parallel to the surface of a uniaxial dielectric. The dielectric surface lies in the $xy$-plane with the optical axis oriented along the $x$-direction. The velocity is $\mathbf{v} = (v_x, v_y, 0) = (v\cos\theta, v\sin\theta, 0)$, where $\theta$ is the angle between $\mathbf{v}$ and the optical axis.

The electromagnetic field due to the moving point charge is calculated from Maxwell's equations:

$$\nabla \cdot \mathbf{D} = \rho, \tag{1}$$

$$\nabla \times \mathbf{H} = \mathbf{J} + \frac{\partial \mathbf{D}}{\partial t}. \tag{2}$$

The problem is tackled by replacing the fields with the standard scalar and vector potentials defined as $\mathbf{B} = \nabla \times \mathbf{A}$ and $\mathbf{E} = -\nabla\Phi - \partial\mathbf{A}/\partial t$. Then the solution to eqs. (1) and (2) is sought separately in the vacuum ($z > 0$) and dielectric ($z < 0$) half spaces by introducing three-dimensional Fourier transforms of all quantities:

$$G(\mathbf{r}, z, t) = \int \frac{\mathrm{d}^2\mathbf{k}\mathrm{d}\omega}{(2\pi)^3} g(\mathbf{k}, z, \omega) e^{i(\mathbf{k}\cdot\mathbf{r} - \omega t)}, \tag{3}$$

where $\mathbf{k} = (k_x, k_y)$ and $\mathbf{r} = (x, y)$ are the wave and position vectors parallel to the dielectric interface.

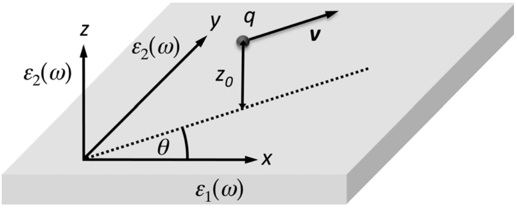


Fig. 1: The point charge moves in vacuum at a distance $z_0$ parallel to the surface of a uniaxial dielectric defined by the $xy$-plane. The velocity makes an angle $\theta$ with the optical axis ($x$-direction). The dielectric tensor is diagonal with $\epsilon_{xx} = \epsilon_1(\omega)$ and $\epsilon_{yy} = \epsilon_{zz} = \epsilon_2(\omega)$.

The absence of bound charges and currents in vacuum allows us to decouple the above equations using the Lorenz gauge:

$$\frac{\partial^2 \Phi_1}{\partial z^2} - Q_1^2 \Phi_1 = -\frac{\rho}{\epsilon_0}, \tag{4}$$

$$\frac{\partial^2 \mathbf{A}_1}{\partial z^2} - Q_1^2 \mathbf{A}_1 = -\frac{\mathbf{J}}{c^2 \epsilon_0}, \tag{5}$$

where $Q_1 = \sqrt{k^2 - \omega^2/c^2}$, $k = \sqrt{k_x^2 + k_y^2}$ is the magnitude of $\mathbf{k}$ and the index 1 refers to the vacuum half space. The Fourier decomposition of the charge density is

$$\rho(\mathbf{k}, z, \omega) = 2\pi q \delta(\omega - \mathbf{v} \cdot \mathbf{k}) \delta(z - z_0), \tag{6}$$

while the current density is simply $\mathbf{J} = \rho \mathbf{v}$.

The solution to eqs. (4) and (5) is written as a sum of the "incident" field due to the point charge (the same as in the absence of the dielectric interface):

$$\Phi_i = \frac{\pi q}{\epsilon_0} \delta(\omega - \mathbf{v} \cdot \mathbf{k}) \frac{e^{-Q_1 |z - z_0|}}{Q_1}, \tag{7}$$

$$\mathbf{A}_i = \frac{\mathbf{v}}{c^2} \Phi_i, \tag{8}$$

and the "scattered" field due to the dielectric

$$\mathbf{A}_s = \mathbf{a}_s e^{-Q_1 z}, \tag{9}$$

where for the latter we impose the gauge $\Phi_s = 0$ and therefore $\nabla \cdot \mathbf{A}_s = 0$.

In these equations $Q_1$ is a real number. This follows from the fact that all the fields carry the prefactor $\delta(\omega - \mathbf{v} \cdot \mathbf{k})$, which insures that $\omega = \mathbf{v} \cdot \mathbf{k}$. Writing $\mathbf{k} = (k \cos\phi, k \sin\phi)$ we obtain $Q_1 = k\sqrt{1 - \beta^2 \cos^2(\theta - \phi)}$, a real quantity for any $\beta = v/c$, $\theta$ and $\phi$. The point charge moving at constant speed parallel to the dielectric surface cannot emit radiation in the vacuum half space —the waves in eqs. (7)–(9) are evanescent and the sign in front of $Q_1$ in eq. (9) is negative to insure that the waves decay to zero as $z \to \infty$

The following linear constitutive relations are assumed for the dielectric: $\mathbf{D} = \epsilon_0 \boldsymbol{\epsilon} \cdot \mathbf{E}$, where $\boldsymbol{\epsilon}$ is diagonal with $\epsilon_{xx} = \epsilon_1(\omega)$ and $\epsilon_{yy} = \epsilon_{zz} = \epsilon_2(\omega)$ and $\mathbf{H} = \mathbf{B}/\mu_0$ (the material is non-magnetic). From eq. (1) we can again set $\Phi_2 = 0$ and therefore $\nabla \cdot (\boldsymbol{\epsilon} \cdot \mathbf{A}_2) = 0$. The equation for the vector potential in the dielectric obtained by taking the curl of eq. (2) then becomes

$$\frac{\partial^2 A_{2x}}{\partial z^2} - Q_{2e}^2 A_{2x} = 0,$$
$$\frac{\partial^2 A_{2y}}{\partial z^2} - Q_{2o}^2 A_{2y} = \left(\frac{\epsilon_1}{\epsilon_2} - 1\right) k_x k_y A_{2x},$$
$$\frac{\partial^2 A_{2z}}{\partial z^2} - Q_{2o}^2 A_{2z} = \left(\frac{\epsilon_1}{\epsilon_2} - 1\right) (-ik_x) \frac{\partial A_{2x}}{\partial z}, \tag{10}$$

where $Q_{2o} = \sqrt{k^2 - \epsilon_2(\omega^2/c^2)} = k\sqrt{1 - \epsilon_2 \beta^2 \cos^2(\theta - \phi)}$ and $Q_{2e} = \sqrt{(\epsilon_1/\epsilon_2) k_x^2 + k_y^2 - \epsilon_1(\omega^2/c^2)} = k\sqrt{\frac{\epsilon_1}{\epsilon_2} \cos^2\phi + \sin^2\phi - \epsilon_1 \beta^2 \cos^2(\theta - \phi)}$, where index 2 (in $Q_{2o,2e}$) refers to the dielectric half space. The above equations are consistent with results obtained by other authors (see, *e.g.* [14,15]), except that we prefer to work with potentials rather than fields.

The general solution to eq. (10) is written as a sum of ordinary (o) and extraordinary (e) waves:

$$\mathbf{A}_2 = \mathbf{a}_o e^{Q_{2o} z} + \mathbf{a}_e e^{Q_{2e} z}, \tag{11}$$

where

$$\mathbf{a}_o = (0, a_{oy}, a_{oz}),$$
$$\mathbf{a}_e = a_e \left(1, \frac{k_x k_y}{k_x^2 - \epsilon_2 \frac{\omega^2}{c^2}}, \frac{-ik_x Q_{2e}}{k_x^2 - \epsilon_2 \frac{\omega^2}{c^2}}\right). \tag{12}$$

Since both $\epsilon_1(\omega)$ and $\epsilon_2(\omega)$ are in general complex quantities, $Q_{2o}$ and $Q_{2e}$ are also complex. There are two solutions for $Q_{2o}$ and $Q_{2e}$ but the physical ones correspond to those with positive real parts (only these decay exponentially in the dielectric and satisfy the radiation condition).

To find the coefficients contained in the vectors $\mathbf{a}_s$, $\mathbf{a}_o$ and $\mathbf{a}_e$ we impose the usual boundary conditions for the fields at the interface. The procedure, although straightforward, is tedious and will not be reproduced in detail. Using the obtained coefficients the Lorentz force components are

$$f_x = iqe^{-Q_1 z_0} \left[\omega a_{sx} + v_y (k_x a_{sy} - k_y a_{sx})\right],$$
$$f_y = iqe^{-Q_1 z_0} \left[\omega a_{sy} + v_x (k_y a_{sx} - k_x a_{sy})\right],$$
$$f_z = -qQ_1 e^{-Q_1 z_0} (v_x a_{sx} + v_y a_{sy}), \tag{13}$$

which become, after the Fourier transform over $\omega$,

$$f_x = -i\frac{k_x}{Q_1} f_z,$$
$$f_y = -i\frac{k_y}{Q_1} f_z,$$
$$f_z = \frac{e^{-2Q_1 z_0} q^2}{2c^2 \epsilon_0} \frac{R}{P}, \tag{14}$$

where $R$ and $P$ are defined as

$$
\begin{aligned}
R = & -\epsilon_2(\mathbf{v}\cdot\mathbf{k})^2\Big\{v_x^2 Q_{2o}(Q_{2e}-Q_1)(Q_{2o}+Q_1) \\
& +v_y^2 Q_{2o}(Q_{2o}-Q_1)(Q_{2e}+Q_1)+2(\epsilon_2-1)k_x k_y v_x v_y Q_1 \\
& +(\epsilon_2-1)k_y^2\Big[v_x^2(Q_{2e}-Q_1)+v_y^2(Q_{2e}+Q_1)\Big]\Big\} \\
& +c^4 k_x^2 Q_{2o}(Q_{2o}+Q_1)(Q_1-\epsilon_2 Q_{2e}) \\
& +c^2\Big\langle 2(\epsilon_2-1)k_x^3 k_y v_x v_y Q_1 \\
& +\epsilon_2 k_y^2 v_y^2(Q_{2e}+Q_1)\Big[Q_{2o}(Q_{2o}-Q_1)+(\epsilon_2-1)k_y^2\Big] \\
& +k_x^2\Big\{Q_1 Q_{2o}\Big[-v_x^2(Q_{2o}+Q_1)+v_y^2(Q_{2o}-Q_1)\Big] \\
& +\epsilon_2 Q_{2o}\Big[v_x^2(2Q_{2e}-Q_1)(Q_{2o}+Q_1)+v_y^2 Q_{2e}(Q_{2o}-Q_1)\Big] \\
& +(\epsilon_2-1)k_y^2\Big[2\left(-v_x^2+v_y^2\right)Q_1+\epsilon_2 v_x^2(Q_{2e}+Q_1)\Big]\Big\} \\
& +2k_x k_y v_x v_y\Big\{(\epsilon_2-1)k_y^2\Big[(\epsilon_2-1)Q_1+\epsilon_2 Q_{2e}\Big] \\
& +Q_{2o}\Big[\epsilon_2 Q_1(Q_{2e}-Q_1)+Q_{2o}(\epsilon_2 Q_{2e}-Q_1)\Big]\Big\}\Big\rangle, \quad (15)
\end{aligned}
$$

$$
\begin{aligned}
P = & \; c^2 k_x^2 Q_{2o}(Q_1+Q_{2o})(Q_1+\epsilon_2 Q_{2e}) \\
& -\epsilon_2(Q_1+Q_{2e})(\mathbf{v}\cdot\mathbf{k})^2\left[Q_{2o}(Q_1+Q_{2o})+k_y^2(\epsilon_2-1)\right]. \quad (16)
\end{aligned}
$$

The force in real space is obtained by integration of the above expressions over $\mathbf{k}=(k\cos\phi, k\sin\phi)$, setting $\mathbf{r}=\mathbf{v}t$. For a lossless and dispersionless material the transform over $k$ is performed analytically, giving an inverse second power dependence of the force on the distance $z_0$ from the surface, while the transform over $\phi$ has to be performed numerically. When dispersion and/or losses are included the integration can be performed only numerically.

The longitudinal force $\mathbf{f}_p=(f_x,f_y)$ can be interpreted in Fourier space in a convenient way. The point particle excites electromagnetic waves in the semi-infinite dielectric and each of these waves carries a momentum proportional to $\mathbf{k}$. This momentum has to be balanced by the particle which results in a force parallel to the interface. The magnitude of the momentum is determined by the boundary conditions and material properties. The longitudinal force $\mathbf{F}_p=(F_x,F_y)$ in real space is then obtained by integration over the momenta of all the excited waves.

In the following we treat two examples of dielectric response: a lossless dielectric with no dispersion and a plasma-type response. Mathematically both cases can be analyzed using the Drude model for the dielectric tensor:

$$
\begin{aligned}
\epsilon_1(\omega) &= \epsilon_{\infty 1}-\frac{\omega_{p1}^2}{\omega(\omega+i\gamma_1)}, \\
\epsilon_2(\omega) &= \epsilon_{\infty 2}-\frac{\omega_{p2}^2}{\omega(\omega+i\gamma_2)}, \quad (17)
\end{aligned}
$$

where $\epsilon_{\infty 1,\infty 2}$ are dielectric constants at high frequencies ($\omega\to\infty$), $\omega_{p1,p2}$ are the plasma frequencies and $\gamma_{1,2}$ are the damping coefficients. For a lossless dielectric $\omega_{p1}$, $\omega_{p2}$ and $\gamma_1$, $\gamma_2$ are made infinitely small, *i.e.* $\epsilon_{1,2}(\omega)=\epsilon_{\infty 1,\infty 2}$, while for a plasma-type dielectric we take $\epsilon_{\infty 1}=\epsilon_{\infty 2}=1$. For reasons of consistency the frequency has to satisfy

$$\omega \gg \gamma_{1,2}. \quad (18)$$

It can be shown (see, *e.g.* [16]) that the range of frequencies a point charge moving above a solid excites near its surface is proportional to $\gamma v/z_0$, where $\gamma=(1-v^2/c^2)^{-1/2}$ is the relativistic factor. The condition of eq. (18) therefore reads

$$\omega_{max}=\frac{\gamma v}{z_0}\gg\gamma_{1,2}. \quad (19)$$

In addition to the above, for non-zero losses the plasma model is not applicable near $\omega_{p1,p2}$, where the imaginary part of the dielectric function dominates the response.

For a lossless dielectric with no dispersion, *i.e.* $\epsilon_1(\omega)=\epsilon_{\infty 1}$ and $\epsilon_2(\omega)=\epsilon_{\infty 2}$ are constants, $\mathbf{F}_p$ will be non-zero only if the Čerenkov condition, either for the ordinary or extraordinary waves (or both), is satisfied. This occurs when either $Q_{2o}$ or $Q_{2e}$ becomes imaginary, *i.e.* the waves become propagating. If both $Q_{2o}$ and $Q_{2e}$ are real, the waves excited in the solid are evanescent (they decay exponentially in the solid) and these do not contribute to $\mathbf{F}_p$. The reason is that $\mathbf{F}_p$ in general decreases the energy of the particle and this can occur only if the charge emits radiation into the dielectric.

It is straightforward to show that $Q_{2o}$ becomes imaginary if the particle moves faster than the critical speed:

$$\beta_o=v_o/c=\frac{1}{\sqrt{\epsilon_2}}. \quad (20)$$

Above $\beta_o$ propagating Čerenkov waves are emitted into a circular cone defined by

$$\cos\alpha_o=\frac{1}{\beta\sqrt{\epsilon_2}}. \quad (21)$$

Here $\alpha_o$ is the angle between the optical axis and the wave vector $\mathbf{K}=(k_x,k_y,\mathrm{sgn}[\omega]k_z)$, and $k_z=iQ_{2o}$. The function $\mathrm{sgn}(\omega)$ insures that the energy flow is directed into the dielectric (propagating waves are actually emitted only into one half of the Čerenkov cone). The symmetry axis of the ordinary Čerenkov cone is always parallel to the particle velocity.

For extraordinary waves the analysis is a bit more cumbersome [17]. The critical speed for Čerenkov emission is

$$\beta_e=\frac{1}{\sqrt{\epsilon_1\sin^2\theta+\epsilon_2\cos^2\theta}}. \quad (22)$$

From eq. (22) it follows that for given $\epsilon_1$, $\epsilon_2$, and $\beta$ there exists a critical angle $\theta_c$ above which the Čerenkov condition for extraordinary waves is satisfied:

$$\cos\theta_c=\frac{1}{\beta}\sqrt{\frac{\beta^2\epsilon_1-1}{\epsilon_1-\epsilon_2}}. \quad (23)$$

$$\tan\chi = \frac{\epsilon_1 - \epsilon_2 + \sqrt{(\epsilon_1-\epsilon_2)^2 + (\beta^2\epsilon_1\epsilon_2)^2 + 2\beta^2\epsilon_1\epsilon_2(\epsilon_2-\epsilon_1)\cos(2\theta)}}{\beta^2\epsilon_1\epsilon_2\sin(2\theta)} - \cot(2\theta), \tag{24}$$

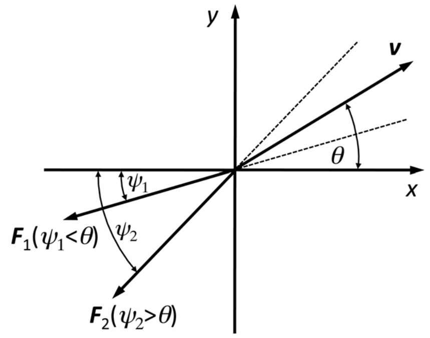


Fig. 2: Different scenarios for the direction of the longitudinal component of the Lorentz force acting on the electron.

The extraordinary Čerenkov cone has an elliptical cross-section [17], which follows from the definition of $Q_{2e}$. The symmetry axis of the cone lies in the $xy$-plane and makes an angle $\chi$ with the $x$-axis[1]:

*see eq.* (24) *above*

which for $\beta=\beta_e$ and $\theta=\theta_c$ reduces to

$$\tan\chi = \frac{\epsilon_1}{\epsilon_2}\tan\theta_c. \tag{25}$$

For a plasma-type dielectric $\mathbf{F}_p$ is in general always non-zero, but is appreciable only in a certain frequency range due to condition (18). This can be seen for the limiting case when $\gamma_1=\gamma_2=0$ and therefore $\epsilon_{1,2}(\omega)=1-\omega_{p1,2}^2/\omega^2$. If follows that $Q_{2o}$ is real for all $\omega$ and there are no ordinary propagating waves. On the other hand, $Q_{2e}$ is imaginary if the frequency $\omega$ lies between the plasma frequencies [18]: *e.g.*, $\omega_{p1}<\omega<\omega_{p2}$ for $\omega_{p2}>\omega_{p1}$. We will refer to this frequency range the Čerenkov band. For zero losses, only waves in the Čerenkov band contribute to the longitudinal force, $\mathbf{F}_p$.

**Results.** – In this section we plot the magnitude of $\mathbf{F}_p$, the angle between $\mathbf{F}_p$ and the electron velocity, and the transverse force $F_z$. For an isotropic material, where $\epsilon_1(\omega)=\epsilon_2(\omega)$, $\mathbf{F}_p$ is in the direction opposite to $\mathbf{v}$, while for a uniaxial material this is no longer the case. We plot $\psi=\arctan(F_y/F_x)$ as a function of $\theta$ to show the effect of the anisotropy (the angle between $\mathbf{v}$ and $\mathbf{F}_p$ is equal to $\psi+\pi$). Figure 2 sketches two possible scenarios that may occur.

[1]To obtain $\chi$ we write the equation for $Q_{2e}$ as $\mathbf{K}\cdot(\mathbf{M}\cdot\mathbf{K})=0$, where $\mathbf{K}=(k_x,k_y,k_z)$, $k_z=iQ_{2e}$ and $\mathbf{M}$ is a $3\times3$ matrix. In the coordinate system where $\mathbf{M}$ is diagonal the equation for $Q_{2e}$ defines the extraordinary Čerenkov cone. The transformation to this coordinate system involves a rotation by $\chi$ along the $z$-axis. The result reduces to the one for ordinary waves when $\epsilon_1=\epsilon_2$.

In fig. 3 we show the results for a dispersionless material with no losses. We chose $\epsilon_1=8$ and $\epsilon_2=4$. On the left side we plot $\psi$ as a function of $\theta$ for different values of $\beta=v/c$, while on the right side we plot the magnitude of the longitudinal force and the transverse force, both normalized with respect to $q^2/(16\pi\epsilon_0 z_0^2)$ (static image charge force for a charge above a metal surface).

The Čerenkov condition for ordinary waves, $\beta_o>0.5$, is only satisfied for bottom panels in fig. 3. For extraordinary waves eq. (23) gives $\theta_c\approx29°$. From fig. 3, $F_p$ is zero below this value and increases with $\theta$. The direction of $\mathbf{F}_p$ strongly departs from the isotropic case and for $\theta=\theta_c$ coincides with the direction of the Čerenkov cone given by eq. (25). This follows directly from eq. (14). For $\theta_c$ the waves are emitted only into one direction (the Čerenkov cone becomes a line); therefore $k_x$ and $k_y$ are proportional and the ratio $F_y/F_x$ is the same as $k_y/k_x$. The longitudinal force is thus parallel to the symmetry axis of the Čerenkov cone. For $\theta>\theta_c$ the direction of $\mathbf{F}_p$ departs from that of the cone.

The transverse force $F_z$ is a result of a complex interplay between evanescent and Čerenkov interactions (see [10,13] for an explanation of the isotropic case); nevertheless, $F_z$ only slightly varies with $\theta$ (within 10% in the interval $\theta\in[0,90°]$). As in the isotropic case [13], $F_z$ is always attractive (negative) for a point charge; it cannot be made repulsive simply by increasing $\beta$ or changing the dielectric constant. However, it can become repulsive by replacing the point charge with a transverse line of charge.

For $\beta=0.5$ the Čerenkov condition for extraordinary waves is satisfied for all $\theta$. For low angles $\psi$ is above the value for the isotropic case: $\psi>\theta$. At some critical angle we enter the regime $\psi<\theta$. Increasing $\theta$ leads to transition back to the regime $\psi>\theta$. This peculiar behavior cannot be qualitatively explained by considering the direction of the Čerenkov cone; the direction of the force has to be determined by integration over all the momenta of the waves excited in the solid.

For higher $\beta$ the Čerenkov condition for ordinary waves is fulfilled. These waves contribute to a force in the direction opposite to the particle velocity. The direction of $\mathbf{F}_p$ therefore approaches that of the isotropic case, as demonstrated in the bottom panels of fig. 3.

We note that for the two extreme points $\theta=0°$ and $\theta=90°$ the longitudinal force always points in the direction opposite to $\mathbf{v}$, which follows from the symmetry of the situation.

As $\beta$ increases the particle excites more Čerenkov waves and therefore the magnitude of $\mathbf{F}_p$ increases, as indicated in fig. 3 (right). For $\beta=0.45$ the maximum value of $F_p$ is $\sim2$ orders of magnitude smaller than $F_z$; however, the components become comparable at $\beta=0.7$.

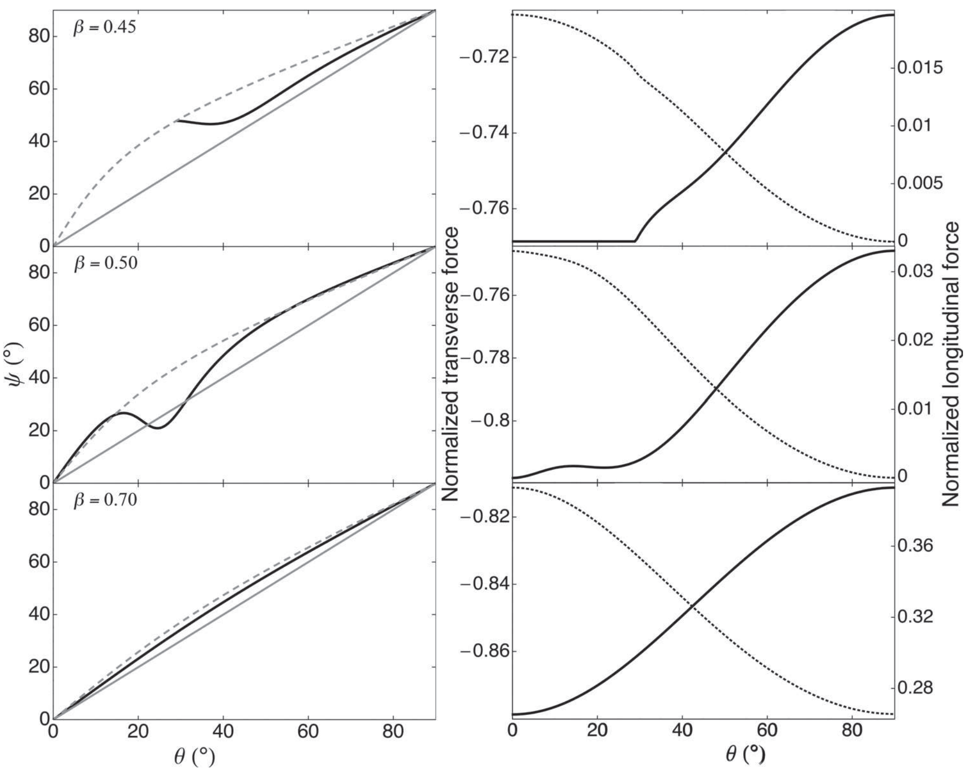


Fig. 3: Results for a dispersionless and lossless dielectric with $\epsilon_1 = 8$ and $\epsilon_2 = 4$. Left: $\psi = \arctan(F_y/F_x)$ as a function of $\theta$ for $\beta = 0.45$ (top), $\beta = 0.5$ (middle) and $\beta = 0.7$ (bottom). The solid black line represents the results, the solid gray line is the isotropic case ($\psi = \theta$, valid for $\beta$ above the Čerenkov condition) and the dashed gray line is the direction $\chi$ of the symmetry axis of the extraordinary Čerenkov cone. Right: magnitude of the longitudinal force (solid line) and transverse force (dashed line) as a function of $\theta$ for $\beta = 0.45$ (top), $\beta = 0.5$ (middle) and $\beta = 0.7$ (bottom).

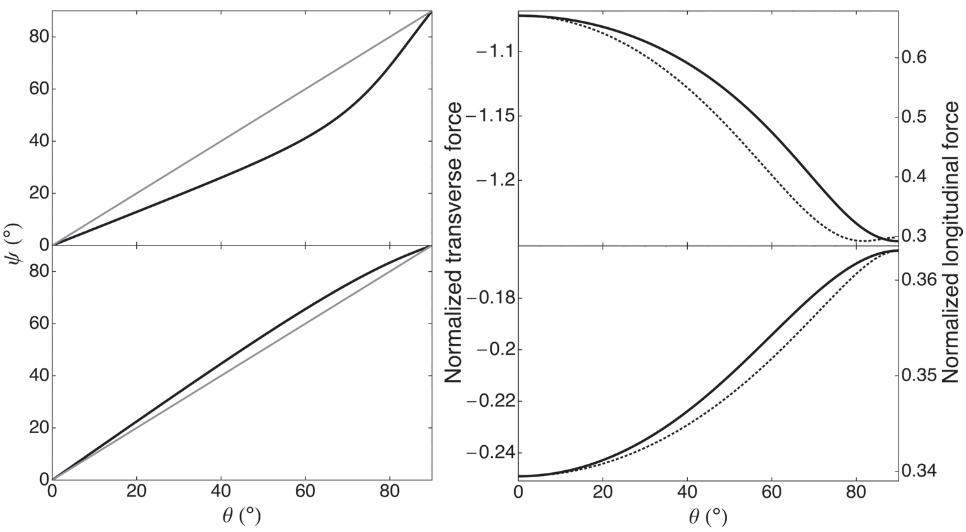


Fig. 4: Results for a plasma-type dielectric ($\gamma_{1,2} = 10^{-2}\omega_{p1}$): $\psi = \arctan(F_y/F_x)$ as a function of $\theta$ (left) and force components (right). Top panels: $\omega_{p2} = 3\omega_{max}$, $\omega_{p1} = 10^{-1}\omega_{p2}$. Bottom panels: $\omega_{p2} = 0.5\omega_{max}$, $\omega_{p1} = 10^{-1}\omega_{p2}$. The solid black line in the left panels represents the results, while the solid gray line is the isotropic case ($\psi = \theta$). The solid line in the right panels is the magnitude of the longitudinal force, while the dotted line represents the transverse force.

For the reversed situation, $\epsilon_1 = 4$ and $\epsilon_2 = 8$, the anisotropy is much less pronounced since with increasing $\beta$ ordinary Čerenkov waves are excited first and these contribute to a force in the direction opposite to $\mathbf{v}$. The effect (not shown here) is similar to the situation in the bottom panel of fig. 3, left, except that $\psi < \theta$.

Figures 4 and 5 show the results for a plasma-type dielectric: $\gamma_{1,2} = 10^{-2} \min(\omega_{p1}, \omega_{p2}, \omega_{max})$. We had to

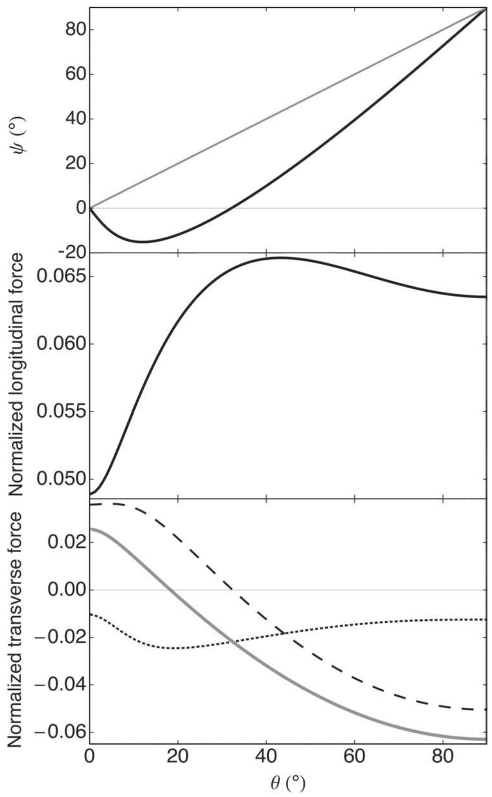


Fig. 5: $\psi = \arctan(F_y/F_x)$ (top panel), magnitude of the longitudinal force (middle panel), and transverse force (bottom panel) as a function of $\theta$ for a plasma-type response with $\omega_{p1} = 0.25\omega_{max}$, $\omega_{p2} = 10^{-1}\omega_{p1}$. The solid black line in the top panel represents the calculated values, the dashed line is the isotropic case. In the bottom panel the transverse force (thick gray line) is split into the Čerenkov (dashed line) and evanescent (dotted line) contributions.

work with finite losses to insure numerical convergence. Although the conditions for a plasma-type dielectric are violated at $\omega = 0$ and near $\omega_{p1,p2}$, insuring that $\omega_{max} \gg \gamma_{1,2}$ and putting the plasma frequencies "far" apart (*e.g.*, $\omega_{p2} = 10\omega_{p1}$), the contribution to the integral around these points is small (the numerical results are nevertheless exact because we are using the Drude model for integration).

Figure 4 demonstrates that the force direction as well as the magnitude change with $\omega_{max}$. Depending on $\omega_{max}$ the angle $\psi < \theta$ or $\psi > \theta$. Since $\omega_{max}$ depends on the particle speed $v$ and the distance $z_0$ from the dielectric, the force magnitude as well as the force direction also depend on $v$ and $z_0$. This is in strong contrast to the case of a dielectric with no losses and no dispersion, where the force direction is independent of $z_0$.

An interesting behavior is observed when $\omega_{max} > \omega_{p1} > \omega_{p2}$, fig. 5. The angle $\psi$ is negative for low $\theta$, which means that the $y$ components of the force and velocity have the same sign and the particle is accelerated in the $y$-direction. Nevertheless, this does not violate energy conservation because the product $\mathbf{v} \cdot \mathbf{F}_p < 0$ and the particle's energy decreases.

A peculiar behavior of the transverse force is observed for values of $\theta$ below $\approx 20°$ where it becomes repulsive (positive). This is shown in the bottom panel of fig. 5, where we split the interaction into the Čerenkov part ($\omega_{p2} < \omega < \omega_{p1}$) and the evanescent part ($0 < \omega < \omega_{p2}$ and $\omega > \omega_{p1}$). For this particular case the Čerenkov contribution, which can become repulsive, starts to dominate for low angles. The origin of the repulsion is the momentum carried into the dielectric by the excited waves, balanced by the particle [10]. It is therefore possible for a dielectric surface not only to repel a transverse charge packet, as demonstrated in ref. [13], but also a point charge; an outcome which seems to contradict common notions based on electrostatic considerations of point charges above metallic or dielectric surfaces.

* * *

The research was in part supported by the Fonds National Suisse (FNS) de la Recherche Scientifique and by the CIBM.

REFERENCES

[1] Morozov A. I., *Sov. Phys. JETP*, **5** (1957) 1028.
[2] Bolotovskii B. M., *Sov. Phys. Usp.*, **4** (1962) 781.
[3] Takimoto N., *Phys. Rev.*, **146** (1966) 366.
[4] Mills D. L., *Phys. Rev. B*, **15** (1977) 763.
[5] Muscat J. P. and Newns D. M., *Surf. Sci.*, **64** (1977) 641.
[6] Barberán N., Echenique P. M. and Viñas J., *J. Phys. C: Solid State Phys.*, **12** (1979) L111.
[7] Mahanty J. and Summerside P., *J. Phys. F: Metal Phys.*, **10** (1980) 1013.
[8] De Zutter D. and De Vleeschauwer D., *J. Appl. Phys.*, **59** (1986) 4146.
[9] Mills D. L., *Solid State Commun.*, **84** (1992) 151.
[10] Schieber D. and Schächter L., *Phys. Rev. E*, **57** (1998) 6008.
[11] Schächter L. and Schieber D., *Nucl. Instrum. Methods A*, **440** (2000) 1.
[12] Schächter L. and Schieber D., *Phys. Lett. A*, **293** (2002) 17.
[13] Rebernik Ribič P, *Phys. Rev. Lett.*, **109** (2012) 244801.
[14] Barash Yu. S., *Radiophys. Quantum Electron.*, **21** (1979) 1138.
[15] Fleck J. A. and Feit M. D., *J. Opt. Soc. Am.*, **73** (1983) 920.
[16] Jackson J. D., *Classical Electrodynamics* (Wiley, New York) 1998, p. 656.
[17] Delbart A., Derré J. and Chipaux R., *Eur. Phys. J. D*, **1** (1998) 109.
[18] Galyamin S. N. and Tyukhtin A. V., *Phys. Rev. E*, **84** (2011) 056608.